

Numerical Analysis of Lateral erosion in bedrock channel based on Discrete Element Method

o Yuze HU, Hokkaido university, Kita-13, Nishi-8, Kita-ku, Sapporo, Japan

E-mail: huyz_civil@yahoo.co.jp

Takuya INOUE, Civil Engineering Research Institute for Cold Region,

1-jo Hiragishi-3, Toyohira-ku, Sapporo, Hokkaido, Japan, E-mail: inoue-t@ceri.go.jp

Yasuyuki SHIMIZU, Hokkaido university, Kita-13, Nishi-8, Kita-ku, Sapporo, Japan

E-mail: yasu@eng.hokudai.ac.jp

The morphology of the bedrock channel is controlled by multiple factors such as sediment feed rate, the properties of the material of both bedrock and sediment, like topography and strength of rock. The abrasion caused by bedload colliding to bedrock has been proved as an important mechanism of erosion on bedrock. The DEM has been applied as a tool to analyze the erosion rate on the metal surface by sand particle collision, which has been proved a good method to simulate the behavior of particles in soil mechanics and powder technology. This study in order to construct a lateral erosion model based on DEM analysis and discuss how the mechanical factors control the bank erosion rate. A comparison between simulation results and experimental data was conducted. The result shows that DEM simulation can predict the location of erosion and the tendency of erosion rate increasing from upstream to downstream.

1. Introduction

As the global warming process, the intense rainfall is more and more frequently all over the world. Intense scouring transported more sediments from upstream to downstream, and then the bedrock was exposed in the upper and middle reaches. Those include channel bed and the foundation of hydraulic structures. Thus, how to estimate the erosion on bedrock has become an essential topic to river management.

An important mechanism of bedrock channel erosion is the incision and abrasion by saltating sediment. (Sklar and Dietrich⁽¹⁾⁽²⁾, 2001, 2004; Finnegan et al.⁽³⁾, 2007; Johnson and Whipple⁽⁴⁾⁽⁵⁾, 2007, 2010; Chatanantavet and Parker, 2009⁽⁶⁾; Inoue et al.⁽⁷⁾, 2014). When bedrock covered by sediments, the lateral erosion on bedrock channel wall was increased where the incision was suppressed (Finnegan et al.⁽³⁾, 2007; Johnson and Whipple⁽⁴⁾⁽⁵⁾, 2007, 2010; Nelson and Seminara⁽⁸⁾, 2011). The detachment caused by the flow shear stress of river (Stark⁽⁹⁾, 2006; Wobus et al.⁽¹⁰⁾, 2006) and the abrasion result from sediment transport (Mishra et al.⁽¹¹⁾, 2018) has been proposed as the factors controlling the lateral erosion of sidewall in bedrock channels. A model proposed by Hancock and Anderson (2002)⁽¹²⁾ in which the erosion rate on bedrock bed is controlled by the rate of sediment transport, but the erosion rate on the sidewall of bedrock channel is also dependent on the stream power. Small et al.⁽¹³⁾ and Inoue et al.⁽¹⁴⁾ suggest that the bedrock strength and the degree of weathering can be two control factors of the erodibility of a bedrock bank.

Inoue et al.⁽¹⁵⁾ have given an approximate solution of permanent form described how a bedrock-alluvial meander bend migrates outward. A parametrically imposed specific sidewall erosion rate with spatiotemporally constant values was used. For clarifying how the sediment feed rate affects lateral erosion on the sidewall of bedrock channels, laboratory experiments and simulations were conducted by Mishra et al. (2016)⁽¹⁶⁾. In those simulations, the lateral erosion rate was parameterized by the lateral sediment transport rate. Two key factors are still vague: The number of collisions between bank and bedload, The lost kinetic energy for every collision. The numerical analysis in the scale of particles is necessary for clarifying these two factors.

Discrete Element Method (DEM)⁽¹⁷⁾ has been proved as an accessible method to describe the behavior of particles in multiphase flow⁽¹⁸⁾. CFD-

DEM with considering the three-dimensional motion of spheres has been used in the analysis of sediment transport.⁽¹⁹⁾

This study aims to analyze the contact force between sidewall and sediments and the energy variation of the contact process, clarify how the sediment affects lateral erosion rate on the sidewall of the bedrock channel in particle scale.

2. Numerical simulation

(1) Flow model

The governing equations for a 2-D plane flow field are based on the numerical model proposed by Asahi et al.⁽²⁰⁾. In computation, the equations were transformed into a boundary-fitted coordinate system. For simplicity here write the equations in an orthogonal coordinate system as follows:

$$\frac{\partial h}{\partial t} + \frac{\partial(hu)}{\partial x} + \frac{\partial(hv)}{\partial y} = 0 \quad (1)$$

$$\frac{\partial(hu)}{\partial t} + \frac{\partial(hu^2)}{\partial x} + \frac{\partial(huv)}{\partial y} = -gh \frac{\partial H}{\partial x} - \frac{\tau_x}{\rho} + D^x \quad (2)$$

$$\frac{\partial(hv)}{\partial t} + \frac{\partial(huv)}{\partial x} + \frac{\partial(hv^2)}{\partial y} = -gh \frac{\partial H}{\partial y} - \frac{\tau_y}{\rho} + D^y \quad (3)$$

where

$$\frac{\tau_x}{\rho} = C_f u \sqrt{u^2 + v^2} \quad (4)$$

$$\frac{\tau_y}{\rho} = C_f v \sqrt{u^2 + v^2} \quad (5)$$

$$D^x = \frac{\partial}{\partial x} \left[v_t h \frac{\partial u}{\partial x} \right] + \frac{\partial}{\partial y} \left[v_t h \frac{\partial u}{\partial y} \right] \quad (6)$$

$$D^y = \frac{\partial}{\partial x} \left[v_t h \frac{\partial v}{\partial x} \right] + \frac{\partial}{\partial y} \left[v_t h \frac{\partial v}{\partial y} \right] \quad (7)$$

in which h is the water depth, t is time, u and v represent velocity, g is the gravitational acceleration, H is water level, C_f is the bed friction coefficient, v_t is an eddy viscosity coefficient calculated by using Von

Karman's coefficient ($\kappa=0.4$), it is given by :

$$v_t = \frac{\kappa}{6}(u_* h) \quad (8)$$

where u_* is the shear velocity.

(2) Model of secondary flow

Considering the effects acted on bedload resulted from secondary flow⁽²¹⁾, The distribution of flow velocity in depth and the traversal is given by:

$$\frac{u_s}{u_*} = \frac{6}{\kappa} \left(\xi - \frac{1}{2} \xi^2 \right) + \left(\varphi - \frac{2}{\kappa} \right) \quad (9)$$

$$u_{nb} = \frac{\beta_s h}{u_*} \left[\frac{u_*^2}{r_s} \left(\frac{24}{5\kappa^2} + \frac{4\beta_s}{\kappa} + \beta_s^2 \right) - g \frac{\partial H}{\partial n} \right] \quad (10)$$

where s is the streamwise direction, n is the normal direction away from the local center of curvature. z is the bi-normal direction in depth. u_s is the flow velocity in s -direction, u_{nb} the velocity in n -direction on bed, r_s is the radius of curve, h is the depth and H the elevation of water. ξ , φ and β_s are given by:

$$\xi = \frac{z}{h} \quad (0 < z < h); \quad \varphi = \frac{\langle u \rangle}{u_*}; \quad \beta_s = \left(\varphi - \frac{2}{\kappa} \right)$$

in which $\langle u \rangle$ is the depth average velocity in s -direction.

The transformation from Cartesian coordinate to the streamwise-normal coordinate refer to the treatment of Asahi et al. ⁽²⁰⁾.

(3) Equations of particle motion

The equations of translational and rotational motion of the particle i are given by:

$$m_i \ddot{x}_i = \sum_j \mathbf{F}_{Cij} + \sum \mathbf{F}_{Oi} \quad (11)$$

$$I_i \dot{\omega}_i = \sum_j \mathbf{M}_{Cij} + \sum \mathbf{M}_{Oi} \quad (12)$$

where m is the mass of particle, I is the particle moment of inertia, the x and ω is the particle position vector and the angular velocity of particle respectively. \mathbf{F}_C and \mathbf{M}_C are the force and torque result from particle contact. \mathbf{F}_O and \mathbf{M}_O are the force result from other factors totally, in this case only considering the drag force from fluid. The equations of fluid drag effects are given by:

$$\mathbf{F}_{f_x} = \frac{1}{2} \rho C_D A_2 d_i^2 \sqrt{(u - u_{pi})^2 + (v - v_{pi})^2} (u - u_{pi}) \quad (13)$$

$$\mathbf{F}_{f_y} = \frac{1}{2} \rho C_D A_2 d_i^2 \sqrt{(u - u_{pi})^2 + (v - v_{pi})^2} (v - v_{pi}) \quad (14)$$

where ρ is density of water. C_D : profile drag coefficient. \mathbf{F}_{f_x} , \mathbf{F}_{f_y} : The fluid resistance on one element in x or y direction. u_{pi} , v_{pi} are the velocity of element i in x or y direction respectively. u , v are the flow velocity where the element i in x or y direction respectively. d_i is the diameter of an element. A_2 is the 2D surface shape factor.

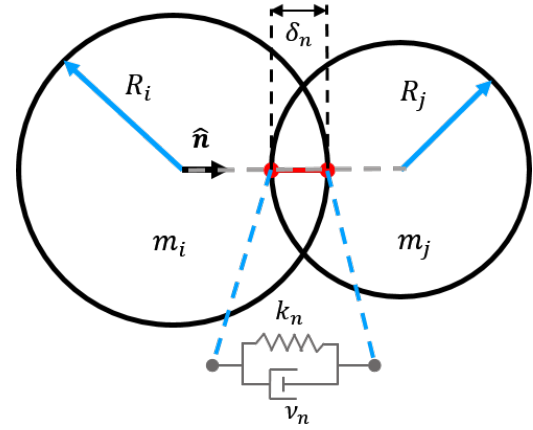


Fig. 1 Contact force model in normal direction

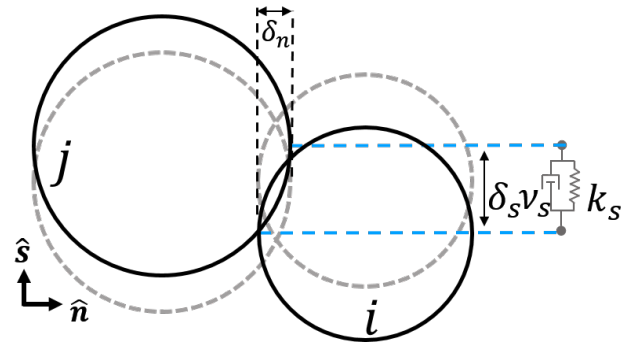


Fig. 2 Contact force model in tangential direction

(4) Contact force model

The Damped Linear Spring (DLS) model⁽¹⁷⁾ was used in simulation, The contact force in normal direction acted on the particle is given by:

$$\mathbf{F}_{N,on_i} = (-k_n \delta_n + \nu_n \dot{\delta}) \hat{n} \quad (15)$$

then the tangential component as follow:

$$\mathbf{F}_{S,on_i} = \min(k_s \delta_s + \nu_s \dot{s}, \mu |\mathbf{F}_{N,on_i}|) \hat{s} \quad (16)$$

where the k_n and k_s is the spring stiffness in the normal direction and tangential direction respectively. ν_n and ν_s is the damping coefficient in the respective direction. δ_n and δ_s , as the fig.1 and fig.2, is the overlap length in the respective direction. $\dot{\delta}$ and \dot{s} is the overlap velocity in the normal and tangential direction respectively. \hat{n} and \hat{s} is the unit vector in the direction marked in fig.1 and 2. The μ is the slide friction coefficient between particle i and j .

The contact between two elements was assumed hertzian⁽²²⁾⁽²³⁾, and the spring stiffness in this model is given by the equivalent maximum strain energy model.⁽²⁴⁾ It is given by:

$$k_n \approx 1.053 (\delta_0 m'^{1/2} R' E')^{2/5} \quad (17)$$

where δ_0 is the relative impact speed. m' , R' and E' is effective mass, effective radius and effective Young's modulus, respectively. They are given by equations as follows:

$$\frac{1}{m'} = \frac{1}{m_i} + \frac{1}{m_j} \quad (18)$$

$$\frac{1}{R'} = \frac{1}{R_i} + \frac{1}{R_j} \quad (19)$$

$$\frac{1}{E'} = \frac{1 - \nu_i^2}{E_i} + \frac{1 - \nu_j^2}{E_j} \quad (20)$$

in which m_i and m_j is the mass of particle i and j , R_i and R_j is the radius of particle i and j , E_i and E_j is the Young's modulus of particle i and j , ν_i and ν_j is Poisson's ratios for i and j , respectively.

The k_s in equation (14) from the elastic solid mechanics analysis of *Mindlin* ⁽²⁵⁾, it is given by:

$$\frac{k_s}{k_n} = \frac{1 - \nu}{1 - 0.5\nu} \quad (21)$$

in which the ν is Poisson's ratios.

In this model, Young's modulus, Poisson's ratios and grain size in those equations were from measurement or experimental data. By this way, the spring stiffness in DLS model is relating to the properties of material.

The damping coefficient ν_n and ν_s in equation (13) and (14) can be obtained by k_n and k_s , they are given by:

$$\nu_n = \sqrt{\frac{4m'k_n}{1 + \beta^2}} \quad (22)$$

$$\nu_s = \sqrt{\frac{4m'k_s}{1 + \beta^2}} \quad (23)$$

where β is given by:

$$\beta = \frac{\pi}{\ln(e)} \quad (24)$$

in which, e is the coefficient of restitution. β also was used to confirm T the contact duration and δ_{max} the max overlap length of the contact between two particles, they are given by:

$$T = \pi \sqrt{\frac{m'}{k_n} \left(1 + \frac{1}{\beta^2}\right)} \quad (25)$$

$$\delta_{max} = \delta_0 \sqrt{\frac{m'}{k_n}} \exp\left[-\frac{\tan^{-1}(\beta)}{\beta}\right] \quad (26)$$

(5) Erosion model

The DEM has been applied to the erosion analysis of metal material, including the elbows of metal pipe⁽²⁶⁾ and the tube erosion in the fluidized bed⁽²⁷⁾. In those, erosion models have been proposed based on the collision angle and velocity⁽²⁸⁾⁽²⁹⁾.

The E/CRC (Erosion/Corrosion Research Center) erosion model⁽²⁹⁾ was used to calculate the erosion rate, it is given by:

$$ER = C(BH)^{-0.59} F_s V_p^n F(\alpha) \quad (27)$$

$$F(\alpha) = \sum_{i=1}^5 A_i \alpha^i \quad (28)$$

Where the ER is erosion ratio defined as the mass removed from the erodible surface divided by the total mass of particles impacting on the surface. The $C = 2.17 \times 10^{-7}$ and $n = 2.41$ are the empirical constants. BH is the Brinell hardness of the material of wall. F_s is a particle shape coefficient, for fully rounded sand particles, it is 0.2. V_p is the particle incidence speed in m/s. α is the particle incidence angle in radians. A_i from $i = 1$ to 5, are 5.40, -10.11, 10.93, -6.33, and 1.43, respectively.

The E/CRC erosion model has been proved as an accurate model in the prediction of erosion rate on metal surface resulted from colliding by sand particles. But as a model designed for metal surface, it cannot be used in predicting the lateral erosion on bedrock directly.

(6) Simulation process

Considering the bedload is moving in a section close to the channel bed. In this simulation, the bottom section is defined by the saltation hop height of sediments proposed by Sklar and Dietrich⁽²⁾, it is given by:

$$\frac{H_s}{d} = 1.44 \left(\frac{\tau^*}{\tau_c^*} - 1\right)^{0.50} \quad (29)$$

where H_s is the hop height of sediments, d the diameter of sediments, τ^* and τ_c^* is Shields number and the critical Shields number respectively.

In this study, we reproduce the flume experiment conducted by Mishra et al. using the one-way coupled DEM described above. Table.1 and Fig. 3 shows the comparison between the experiment and the simulation and the shape of the flume, respectively.

The erosion width (W_l) was calculated as follow:

$$W_l = \beta_m \frac{2}{3} d \frac{\rho_s}{\rho_{wall}} \frac{N_o T_o}{N_s T_s} ER \quad (30)$$

where β_m is related to the difference of material properties between bedrock and metal, in this simulation the β_m is set as a constant 5. d is the diameter of sediment; The ρ_s and ρ_{wall} the density of the sediment and channel wall respectively. N_o and T_o , respectively, the sediment feed rate and the duration of the original condition in the experiment, and N_s , T_s are the same parameters in the simulation.

	Experiment	Simulation
Grain diameter size	0.74 mm	0.74 mm
Width of flume	5 cm	5 cm
Wave number of flume	3	3
Wavelength of flume	100 cm	100 cm
Slope of flume	0.01	0.01
Meanderangle of flume	60 degree	60 degree
Discharge of water (m ³ /s)	0.0005	0.0005
Time	4 hours	12 seconds
Sediment feed rate (m ² /s)	1.7*10 ⁻⁵	1.06*10 ⁻⁷

Table. 1 Comparison of conditions

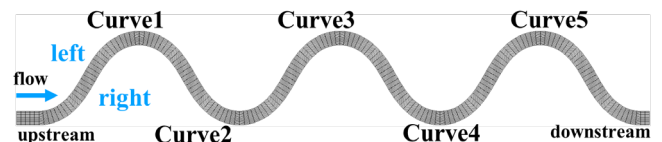


Fig. 3 The shape of flume

3. Result

Apply the DEM model and erosion model referred above. The data from the experiment conducted by Mishra et al. ⁽¹⁶⁾. To compare the result from DEM simulation and the experimental data from Mishra et al. ⁽¹⁶⁾, as shown as Fig.4, 5, and 6. The result of DEM simulation shows the same tendency as the experiment: from upstream to downstream, The lateral erosion rate is increasing.

The simulation results of the bank erosion width are well agreement with the experimental results (Figs. 4 and 8). The erosion width increases from upstream to downstream in both previous experiment and our simulation. However, which factor makes the erosion rate increased from upstream to downstream is still not clear. Therefore, we investigate the following three factors: 1. Collision angle, 2. The average speed of the particle group. 3. The distribution of particles in the transversal. Where the third factor is a non-dimensional quantity σ_t , it is the standard deviation of the non-dimensional particle transversal position. σ_t is given by the equation as follow:

$$\sigma_t = \frac{\sum_{i=1}^N |p_t(i) - \bar{p}_t|}{N}; \quad \bar{p}_t = \frac{1}{N} \sum_{i=1}^N p_t(i) \quad (31)$$

where N is the amount of traced particles. i means the number of particle. $p_t(i)$ is the non-dimensional position of particle i in transversal, it should be a value from 0 to 1. \bar{p}_t is the average value of p_t .

The distribution of those three values along the centerline of the flume is shown as Fig.8, 9, and 10. In which, the average speed of particles shows an increasing tendency. The figure also shows the group speed lost on the curves, which means the kinetic energy of particles was lost there. Fig.8, the factor of transversal distribution shows a tendency that when the particles group passed a curve, particles were concentrated in transversal, which makes collisions occurred more concentrated. The result shows these two factors partly controlled the bank erosion rate, and they were working together in the abrasion process.

Conclusions

This study using the experimental results of Mishra et al. ⁽¹⁶⁾, based on the DEM simulation and a semi-empirical erosion model ⁽²⁹⁾, analyzed the variation tendency of bank erosion rate from upstream to downstream. Mainly discussed how the two factors changed in the process: The average speed of the particle group and the transversal distribution of particles.

DEM model shows intuitive and interpretable, but it also needs high accurate measurement in experiments to get the parameters such as material properties. From this study, It was found in DEM simulation that two controlling factors acted on the bank erosion rate together, the group speed of particles and the distribution of collisions. However, it is clear that the DEM simulation in such a short time cannot get a result of the bank erosion rate in high accuracy. The next step is to combine the parameterized erosion model with the DEM model. Take the change of flume width into considering, to build the erosion model for different bedrock material.

Acknowledgment

The first author would like to acknowledge Dr. Iwasaki, Associate professor of the Faculty of Engineering, Hokkaido University, for the advice on both simulation conditions and the format of the paper.

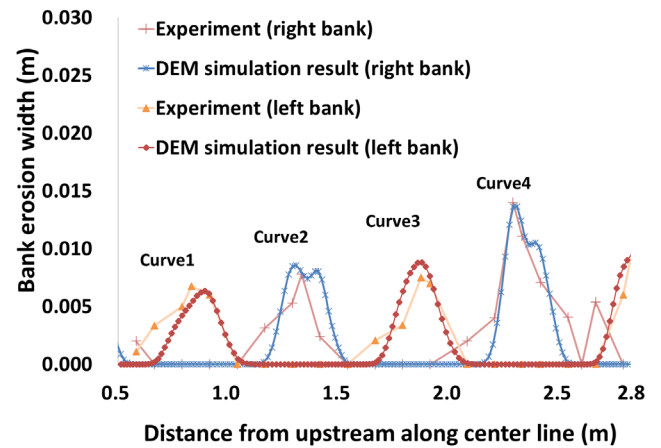


Fig. 4 The comparison of bank erosion width both sides

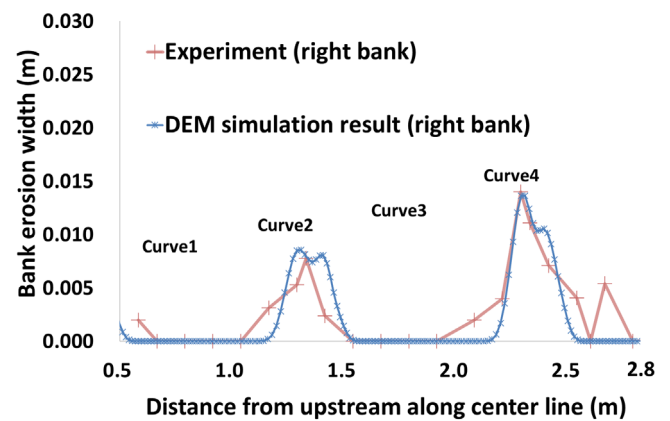


Fig. 5 The comparison of erosion width on right bank

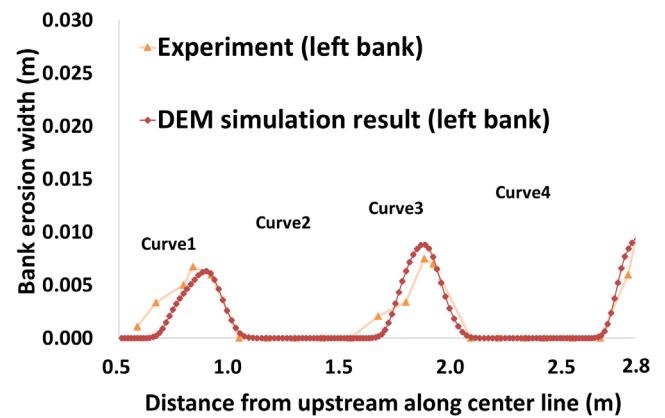


Fig. 6 The comparison of erosion width on left bank

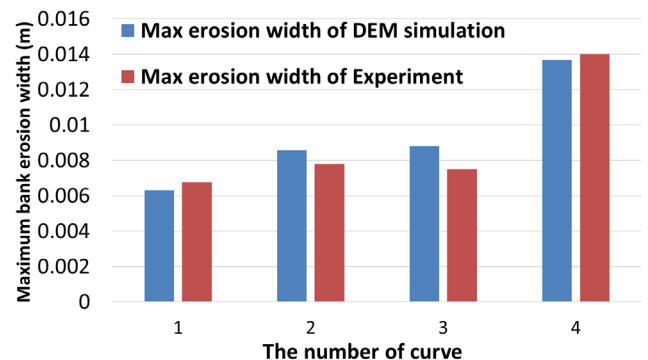


Fig. 7 The comparison of maximum erosion width

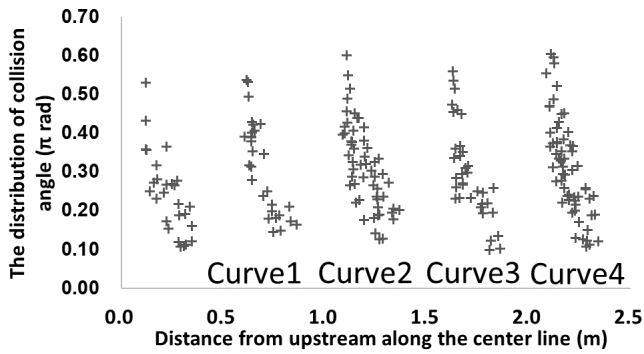


Fig. 8 The distribution of collision angle

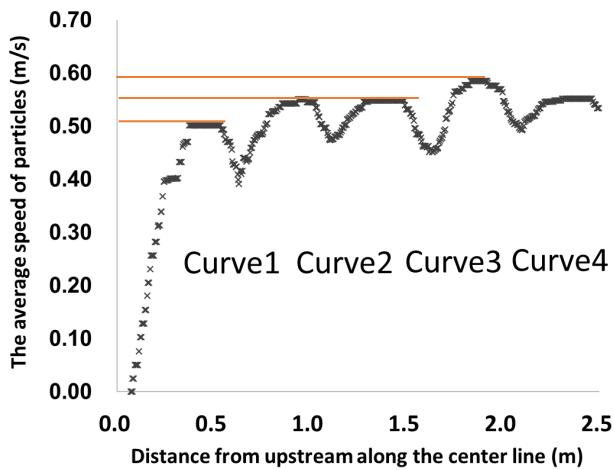


Fig. 9 The average speed of particles

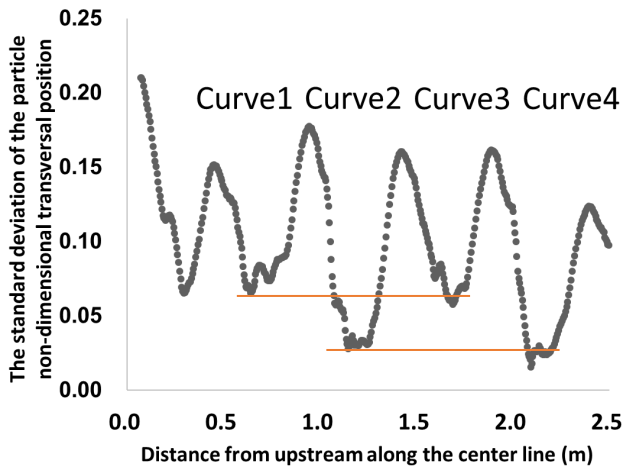


Fig. 10 Standard deviation of dimensionless transversal position

References

- (1) Sklar LS, Dietrich WE., "Sediment and rock strength controls on river incision into bedrock." *Geology* 29(2001), pp.1087-1090.
- (2) Sklar LS, Dietrich WE., "A mechanistic model for river incision into bedrock by saltating bed load." *Water Resources Research* 40(2004), pp. W06301.
- (3) Finnegan NJ, Sklar LS, Fuller TK., "Interplay of sediment supply, river incision, and channel morphology revealed by the transient evolution of an experimental bedrock channel." *Journal of Geophysical Research* 112 (2007), pp. F03S11.
- (4) Johnson JP, Whipple KX., "Feedbacks between erosion and sediment transport in experimental bedrock channels." *Earth Surface Processes and Landforms* 32 (2007), pp.1048-1062.
- (5) Johnson JP, Whipple KX., "Evaluating the controls of shear stress, sediment supply, alluvial cover, and channel morphology on experimental bedrock incision rate." *Journal of Geophysical Research* 115 (2010), pp. F02018
- (6) Chatanantavet P, Parker G., "Physically based modeling of bedrock incision by abrasion, plucking, and macroabrasion." *Journal of Geophysical Research* 114 (2009), pp. F04018.
- (7) Inoue T, Izumi N, Shimizu Y, Parker G., "Interaction among alluvial cover, bed roughness, and incision rate in purely bedrock and alluvial-bedrock channel." *Journal of Geophysical Research - Earth Surface* 119 (2014), pp.2123-2146.
- (8) Nelson PA, Seminara G., "Modeling the evolution of bedrock channel shape with erosion from saltating bed load." *Geophysical Research Letters* 38 (2011), pp. L17406.
- (9) Stark CP., "A self-regulating model of bedrock river channel geometry." *Geophysical Research Letters* 33 (2006), pp. L04402.
- (10) Wobus CW, Tucker GE, Anderson RS., "Self-formed bedrock channels." *Geophysical Research Letters* 33 (2006), pp. L18408.
- (11) Jagriti Mishra, Takuya Inoue, Yasuyuki Shimizu, Tamaki Sumner, Jonathan M. Nelson., "Consequences of Abrading Bed Load on Vertical and Lateral Bedrock Erosion in a Curved Experimental Channel." *Journal of Geophysical Research: Earth Surface* Vol. 123 (2018), pp.3147-3161.
- (12) Hancock GS, Anderson RS., "Numerical modeling of fluvial strath-terrace formation in response to oscillating climate." *Geological Society of America Bulletin* 114 (2002), pp.1131-1142.
- (13) Eric E. Small, Tevis Blom, Gregory S. Hancock, Brian M. Hynek, and Cameron W. Wobus., "Variability of rock erodibility in bedrock - floored stream channels based on abrasion mill experiments." *Journal of Geophysical Research: Earth Surface* Vol. 120 (2015), pp.1455-1469.
- (14) Takuya Inoue, Satomi Yamaguchi, Jonathan M. Nelson., "The effect of wet-dry weathering on the rate of bedrock river channel erosion by saltating gravel." *Geomorphology* Vol. 285(2017), pp.152-161.
- (15) Inoue T, Iwasaki T, Parker G, Shimizu Y, Izumi N, Stark CP, Funaki J., "Numerical simulation of effects of sediment supply on bedrock channel morphology." *Journal of Hydraulic Engineering* Vol. 142 (2016), pp. 04016014.
- (16) Mishra J, Inoue T, Shimizu Y., "Simulations of Lateral Erosion in Bedrock Channels." *Journal of applied mechanics : JSCE* Vol. 19 (2016), pp. 527-536.
- (17) P.A. Cundall, O.D.L. Strack., "Discrete numerical model for granular assemblies." *Geotechnique* 29-1 (1979), pp. 47-65.
- (18) Tsuji, Y., Tanaka, T. and Ishida, T., "Lagrangian numerical simulation of plug flow of cohesionless particles in a horizontal pipe." *Powder Technology* Vol. 71 (1992), pp. 239-250.
- (19) Masato SEKINE., "Numerical simulation of gravel bed deformation on the basis of particle motion analysis." *Proceedings of hydraulic engineering* Vol. 49 (2005), pp. 973-978.
- (20) Asahi, K., Y. Shimizu, J. Nelson, and G. Parker., "Numerical simulation of river meandering with self-evolving banks." *J. Geophys. Res. Earth Surf.*, Vol. 118 (2013), pp. 2208-2229.
- (21) Helgi Johannesson and Gary Parker., "Secondary Flow in Mildly Sinuous Channel." *Journal of Hydraulic Engineering*, Vol. 115 (1989), pp. 289-308.

- (22) Hertz, H., "Über die Berührung fester elastischer Körper.", *J. reine und angewandte Mathematik*, Vol. 92 (1882), pp. 156-171.
- (23) Johnson, K.L., "Contact Mechanics.", Cambridge University Press (1985).
- (24) Lan, Y. and Rosato, A.D., "Macroscopic behavior of vibrating beds of smooth inelastic spheres.", *Physics of Fluids*, Vol. 7, No. 8 (1995), pp. 1818-1831.
- (25) Mindlin, R. D., "Compliance of Elastic Bodies in Contact.", *Journal of Applied Mechanics*, Vol. 16 (1949), pp. 259-268.
- (26) Jukai Chen, Yueshe Wang, Xiufen Li, Renyang He, Shuang Han, Yanlin Chen., "Erosion prediction of liquid-particle two-phase flow in pipeline elbows via CFD-DEM coupling method.", *Powder Technology*, Vol. 275 (2015), pp. 182-187.
- (27) Yongzhi Zhao, Lei Xu, and Jinyang Zheng., "CFD-DEM Simulation of Tube Erosion in a Fluidized Bed.", *AIChE Journal*, Vol. 63 (2017), pp. 418-437.
- (28) Lei Xu, Qian Zhang, Jinyang Zheng, Yongzhi Zhao., "Numerical prediction of erosion in elbow based on CFD-DEM simulation.", *Powder Technology*, Vol. 302 (2016), pp. 236-246.
- (29) Y. Zhang, E.P. Reuterfors, B.S. McLaury, S.A. Shirazi, E. Rybicki., "Comparison of computed and measured particle velocities and erosion in water and air flows.", *Wear*, Vol. 263 (2007), pp. 330-338.